Comparison of auditory evoked potential thresholds in three species of sharks

Carolin Nieder*, Jimmy Rapson, John Montgomery, Craig Radford

Institute of Marine Science, University of Auckland, Leigh Marine Research Laboratory, 160 Goat Island Road, Leigh, Auckland 0985, New Zealand

*Author for correspondence: cnie398@aucklanduni.ac.nz

Abstract

Auditory sensitivity measurements have been published for only 12 of the more than 1,150 extant species of elasmobranchs (sharks, skates, and rays). As a result, there is the need to further understand sound perception in more species from different ecological niches. In this study the auditory evoked potential (AEP) technique was used to compare hearing abilities of the bottom-dwelling New Zealand carpet shark *Cephaloscyllium isabellum*, and two benthopelagic houndsharks (Triakidae), rig *Mustelus lenticulatus*, and school shark *Galeorhinus galeus*. AEPs were measured in response to tone bursts (frequencies: 80, 100, 150, 200, 300, 450, 600, 800, and 1200Hz) from an underwater speaker positioned 55cm in front of the shark in an experimental tank. AEP-detection thresholds were derived visually and statistically, with statistical measures slightly more sensitive (average~4dB) than visual methodology. Hearing abilities differed between species, mainly with respect to bandwidth rather than sensitivity. Hearing was least developed in the benthic *C. isabellum* [upper limit: 300Hz, best hearing: 100Hz (82.3+1.5 dB re:1µms^{-2})]. Hearing was superior in the benthopelagic rig and school sharks [upper limit: 800Hz, best hearing: 100Hz (79.2+1.6 dB re:1µms^{-2}) for *G. galeus*, and 150Hz (74.8+1.8 dB re:1µms^{-2}) for *M. lenticulatus*]. The data are consistent with those known for 'hearing non-specialist' teleost fishes that only detect particle motion, not pressure. Further, our results provide evidence that benthopelagic sharks exploit higher frequencies (max.800Hz) than some of the bottom-dwelling sharks

(max.300Hz). Further behavioural and morphological studies are needed to identify what ecological factors drive differences in upper frequency limits of hearing in elasmobranchs.

Keywords: Elasmobranchs, hearing sensitivity, electrophysiology, New Zealand carpet shark, *Cephaloscyllium isabellum*, rig shark, *Mustelus lenticulatus*, school shark, *Galeorhinus galeus*

Introduction

Elasmobranchs (sharks, skates, and rays) are generally regarded as having a poor sense of hearing. This perception is based upon the relativity poor acoustic sensitivity and narrow frequency detection bandwidth (<1 kHz) compared to most teleosts (Maisey & Lane, 2010; Popper, Hawkins, & Sisneros, 2021). Auditory research in elasmobranchs has received little attention, with basic acoustic sensitivity measurements published for only 12 of the more than 1,150 extant species of elasmobranch (Chapuis & Collin, 2022; Ebert, Dando, & Fowler, 2021; Wiernicki et al., 2020). Yet, sound may be of greater importance to this ancient, and diverse group of fishes than previously thought. Behavioural evidence suggests that elasmobranchs use sound for prey detection (Backus, 1963; Banner, 1972; Myrberg, 1972; Myrberg, Gordon, & Klimley, 1976; Nelson & Gruber, 1963; Nelson & Johnson, 1970; Richard, 1968), predator avoidance (Chapuis et al., 2019; Fetterplace et al., 2022; Klimley & Myrberg, 1979; Myrberg, Gordon, & Klimley, 1978), and potentially reproduction (Carrier, Pratt, & Martin, 1994). Despite the behavioural evidence there is relatively little physiological data on understanding sound perception in elasmobranchs and their close relatives (Chapuis & Collin, 2022; Mickle & Higgs, 2022).

Underwater sound consists of two components, sound pressure, which is a scalar and omnidirectional; and particle motion, which is a vector and directional (Rogers & Cox, 1988). In fish the lateral line and the inner ear detect particle motion (Kalmijn, 1988). The ear has three semi-circular canals that are involved in determining the angular movements of the fish (Lowenstein, 1971). The ear also has three otoconial organs, the saccule, lagena, and utricle, that are involved in both determining the orientation of the fish relative to gravity and detecting sound (Lowenstein & Roberts, 1950; Lowenstein & Roberts, 1951). (Corwin,

1981b; Kalmijn, 1988; Popper & Fay, 1977). The otoconial endorgans contain sensory epithelia (maculae) composed of supporting cells and sensory hair cells that are overlain by a dense otoconial mass (Mulligan & Gauldie, 1989) (Mulligan & Gauldie, 1989; Tester, Kendall, & Milisen, 1972). At the apical ends of the hair cells are ciliary bundles, composed of many stereocilia that are organized in a stepwise arrangement of increasing height, leading to a single kinocilium (Flock, 1971). The vibrations generated by a sound source efficiently propagate through the water and move the fish as water and fish have similar densities (Rogers & Cox, 1988). The denser otoconia lag the motions of surrounding soft tissue, and bend the hair cell bundles, which activates the auditory system (Flock & Wersall, 1963). Fishes with internal gas-filled structures (e.g., swim bladder, auditory bullae, branchial bubbles) can detect sound pressure (Popper and Fay, 1999). The vibrations of the gas bubble transform the pressure signal into particle motion, which is then transmitted to the inner ear (Sand & Enger, 1973). Elasmobranchs lack any known pressure transducing structure; therefore, it is thought that they can only detect the particle motion component of the sound field (Banner, 1967; Kelly & Nelson, 1975; Popper & Hawkins, 2021).

Elasmobranchs also detect sound using a fourth endorgan that is not loaded with an otoconial mass, the macula neglecta, located inside the posterior canal duct (Corwin, 1977; Corwin, 1981b; Fay et al., 1974; Lowenstein & Roberts, 1951; Retzius, 1881). The macula neglecta is particularly well developed in sharks and is thought to function in directional hearing in carcharhinid sharks (Corwin, 1977; Corwin, 1978). The hair cells are embedded in a gelatinous cupula, which is suspended in the endolymphatic fluid of the posterior canal duct (Tester et al., 1972). The hair cells of the macula neglecta are very likely stimulated by movements of the cupula (Tester et al., 1972), however the modus operandi, including the adequate stimulus have not been unequivocally demonstrated (Popper & Fay, 2011).

Regardless of the mechanism, when bent in the appropriate direction, the sensory hair cells of the otoconial endorgans and the macula neglecta, convert acoustic energy into electric potentials that can be measured from the eighth nerve and higher auditory centres in the brainstem (Bullock & Corwin, 1979; Fay & Popper, 2000; Flock & Wersall, 1963). The auditory evoked potential (AEP) technique has commonly been used to measure basic acoustic abilities in fish (Ladich & Fay, 2013), including sharks (Bullock & Corwin, 1979; Casper & Mann, 2009; Corwin, Bullock, & Schweitzer, 1982). It is a relatively quick, non-invasive method to record compound field potentials of the entire auditory system (Bullock & Corwin, 1979; Corwin et al., 1982; Kenyon, Ladich, & Yan, 1998). The method has its

limitations, because hearing is a complex cognitive process that requires signal integration at the level of the whole animal and the AEP technique only represents one part of that (Popper et al., 2019; Popper & Hawkins, 2021). Nonetheless, the AEP technique has proven extremely useful to compare frequency detection range and best sensitivity among different species (Ladich & Fay, 2013; Vetter, Brey, & Mensinger, 2018; Wysocki et al., 2009). A review (Ladich & Fay, 2013) of AEP generated detection threshold curves only includes two species of rays, and six species of sharks, highlighting the need to assess more species from different families, habitats, and ecological roles.

The goal of this study was to measure auditory detection thresholds in the New Zealand carpet shark (*Cephaloscyllium isabellum;* Bonnaterre, 1788), the rig shark (*Mustelus lenticulatus;* Phillipps, 1932), and the school shark (*Galeorhinus galeus;* Linnaeus, 1758) using the AEP technique in combination with an underwater speaker tank setup. The carpet shark is a nocturnal, slow swimming, benthic shark. The benthopelagic rig shark swims most of the time and specialises on crushing crustaceans close to the seafloor (Francis et al., 2012). The school shark is a benthopelagic species that continuously swims and preys on small fishes and invertebrates (Francis & Mulligan, 1998). The results of the present study extend current knowledge of elasmobranch hearing abilities and will be useful for future integration with morphological and behavioural studies.

Material and methods

Animal collection and husbandry

Six rig (3 male, 3 female, TL range 51.5-70 cm) and seven school sharks (4 male, 3 female, TL range 49.5-75 cm) were caught using circle-hook and line in the Kaipara Harbour (New Zealand, North Island). Eight carpet sharks (5 male, 3 female, TL range 58.5-75 cm) were obtained from local commercial fishermen (

Table). Animals were housed in flow-through holding tanks, supplied with ambient seawater, and maintained on a mixed diet of squid and fish three times a week. Sharks were acclimated for at least one week prior to experimentation. All procedures were conducted in accordance with ethics protocols #002066/#AEC23071, approved by the University of Auckland Animal Ethics Committee (AEC).

Tank setup, stimulus generation

A 4360 L circular tank (made of high-density polyethylene, 2100 mm inside diameter, 1260 mm water depth) was isolated from ground vibrations by sitting on rubber tyres. A monopole underwater loudspeaker (UW-30, Lubell Labs Inc., Columbus, OH, USA) was wrapped in tinfoil and grounded to reduce signal interference during AEP recordings. The speaker was suspended from a wooden plank using nylon and bungee cords and positioned in the centre of the tank 65 cm below the surface (Fig. 1). The plank was isolated from the tank with multiple sheets of vibration and noise dampening mats. The water temperature and salinity ranged from 14.7 to 22.5 $^{\circ}$C and 35 to 36 ppt, respectively.

Auditory stimuli were produced by a sound module (Tucker-Davis Technologies, TDT, Gainesville, FL, USA) operated by a laptop (Lenovo ThinkPad X270) running SigGen® (version 4.4.9) and BioSig® (version 4.4.11) software. Signals were digitised (RP 2.1, TDT) attenuated (PA5, TDT) and amplified (Pyle®, PLA2378, Sonic Electronix, Louisville, KY USA) before being played through the speaker. Auditory signals consisted of pulsed tone bursts (25-50 ms duration, with a 3 ms rise/ fall time gated through a Hanning window) at 80, 100, 150, 200, 300, 450, 600, 800 and 1200 Hz (Table). The frequency specificity of acoustic tone pips in confined tank setups can depend on the stimulus duration (e.g., Christensen, Christensen-Dalsgaard, & Madsen, 2015; Lauridsen, Brandt, & Christensen-Dalsgaard, 2021). Initial examinations of the frequency spectra of all test stimuli in our tank setup revealed that optimal frequency specificity was achieved for pip durations of 50 ms for the lower frequency tone-bursts (<450 Hz), and 25 ms for frequencies 450-1200 Hz. Pressure waveforms, spectral levels and particle acceleration magnitude spectra are shown in Figure 2.

Acoustic evoked potential measurements

Prior to experiments the shark was anesthetized by immersion (~10-15 min) in a salt-water bath of MS-222 (Ethyl 3-aminobenzoate methanesulfonate, PubChem Substance ID: 24894382, Sigma Aldrich) and sodium hydrogen bicarbonate in a 1:2 ratio. When there was no response to tail-pinching the shark was firmly wrapped (from pectoral fins to tail, leaving the gills exposed for breathing to occur normally) into a piece of stocking, and positioned ventrally onto a custom-made plastic mesh holder, where it was secured with velcro straps. Stainless steel reusable subdermal needle electrodes (27-gauge, 13 mm, Rochester Electromedical Inc.; Coral Springs, FL, USA) were used to record AEPs. The recording electrode was inserted dorsally, underneath the skin, at the border of the largest lateral-medial diameter of the parietal fossa. The reference electrode was inserted into the cartilage at the tip of the snout, and the ground electrode was placed in plasticine next to the shark's body. The electrodes were insulated with nail varnish, apart from the tips. The electrode wires were tightly wrapped in tinfoil tape and surrounded by a grounded stainless steel mesh sleeve to minimise interference and electrical noise.

The animal holder was then carefully lowered into the tank to ~70 cm under the waterline, such that the inner ear of the shark was positioned 55 cm in front, and 5 cm above the underwater speaker (Figure 1). Carpet and rig sharks are buccal pumpers, therefore were allowed to recover from the initial anaesthesia. School sharks are ram ventilations and therefore were required to be ventilated with a dilute mixture of anaesthetic (0.075 g/l MS-222 and 0.115 g/l sodium hydrogen bicarbonate) that was dripped through the mouth and over the gills during the experiment to maintain a mild anaesthetised state. Previous research (Chapius et al 2017) has shown that MS222 has no significant effect on the shark's AEP responses at the concentrations used in this study. The presentation order of the frequencies was conducted randomly. An average of 1200 responses (600 sweeps from stimuli presented at 0^{o} and 600 sweeps from stimuli presented at 180^{o}) was taken for each sound pressure level (SPL) at each frequency. However, to verify AEPs close to threshold level 2000 sweeps were undertaken (e.g., 1000 sweeps at each polarity). AEPs were first elicited using a SPL above threshold (Table). The SPLs were then decreased in 5 dB steps for each frequency until an AEP could no longer be visually identified. Then, one to three additional measurements, at 5-15 dB below this roughly estimated threshold were made to ensure responses were not missed. The presence of an AEP was verified visually through 1) observation of the characteristic wave visible above the background noise, and 2) by FFT analysis to screen for

peaks at twice the stimulus frequency. This method is commonly used in fish AEP studies (Casper, Lobel, & Yan, 2003; Kenyon et al., 1998) and is based on the theory that the opposed orientation of the hair cells in the sacculus of the inner ear gives rise to the characteristic frequency response at twice the stimulus frequency (Fay, 1974). The visual estimate of the hearing threshold was defined as the lowest SPL that generated an AEP response in both the averaged trace and the FFT (Vetter et al., 2018).

Dead controls (10 in total) were frozen for a minimum of 24 hours and defrosted prior to the control experiment. Control experiments were run according to the same protocol, including the positioning of the electrodes. No AEPs were elicited from any of these control specimens confirming that the AEPs recorded in this study represent electrophysiological responses from live sharks and were no artefacts from the experimental setup.

Objective estimation of hearing thresholds

As suggested by Sisneros et al. (2016) we included an objective AEP threshold determination method, because visual methods alone were shown to be subject to observer bias (Xiao & Braun, 2008). The 'x-intercept' estimation method applied here has previously been used in hearing studies with marine mammals (Nachtigall et al., 2004; Nachtigall et al., 2007), cephalopods (Mooney et al., 2010), and crustaceans (Dinh & Radford, 2021; Jézéquel et al., 2021). First, the 2048-point fast Fourier transform (FFT) power spectra was calculated for five to twelve averaged waveforms per frequency, using a custom-written MATLAB script (see Figure 5 for example). As with fish AEPs, the spectra revealed peaks at twice the stimulus frequency at suprathreshold, and a decrease in FFT peak amplitude corresponded with decreasing SPLs (Maruska & Sisneros, 2016). Second, the maximum FFT values (peak value) were found across five FFT bins greater than, and five FFT bins less than twice the presented frequencies and were plotted against the presented SPL (see panel d) of Figure 5. Third, a series of regressions was run, that included 3, then 4, 5, to the ith peak value. The regression line that yielded the highest r^2-value (best fitting line) was selected to calculate the x-intercept. The x-intercept of the best fitting line served as estimate of the animal's probable hearing threshold (Nachtigall et al., 2007).

Pressure and particle acceleration calibrations

Acoustic stimuli were calibrated at the beginning of every experimental day using a miniature reference hydrophone (TC4013, sensitivity -211 dB re 1 VμPa^{-1}, Teledyne Reson Ltd, Slangerup, Denmark) placed inside the empty animal holder and held in place by rubber bands at the same location where the animal's inner ear would be located during the experiment. A digital oscilloscope (Tektronix DPO2014 digital phosphor oscilloscope) was used to measure the sound pressure level (SPL) at each frequency, which was then attenuated through SigGen to output the desired decibel levels. Filtered ambient noise readings were taken to ensure that background sound levels were similar between test days.

Acoustic particle motion is likely the most relevant stimulus for hearing in sharks, we subsequently measured the particle acceleration levels, associated with each determined pressure threshold. A waterproofed triaxial accelerometer (DeltaTron®, Type 4524, National Instruments, Austin, TX, USA; sensitivities: x = 9.770 mV/ms^{-2}, y = 9.977 mV/ms^{-2}, z = 10.02 mV/ms^{-2}) was placed into the fish holder and held in place by rubber bands in the position of the shark's inner ear. The sensors were aligned such that 'x' would be the along-body axis (head to tail), 'y' the left-right axis and the 'z' was the vertical axis. Data from the accelerometer were amplified with a Brüel & Kjær signal conditioning amplifier (NEXUS Type 2690-OS4, Nærum, Denmark) and the peak-to-peak voltage ($V_{pk\text{-}pk}$) measured on an oscilloscope (Tektronix DPO 2014). The $V_{pk\text{-}pk}$ was converted to V_{rms} and the acceleration was calculated for the x, y, and z planes and followed by the particle acceleration magnitude (μms^{-2}, calculated as $\sqrt{x^2 + y^2 + z^2}$).

Acoustic impedance measurements

As suggested by Popper et al., (2019) and Popper and Fay (2011) we report the acoustic impedance of the testing environment for all stimulus frequencies and compare it to the acoustic impedance in water in a free field. The acoustic impedance is defined as the ratio between sound pressure [Pa] and particle velocity [ms^{-2}]. In contrast to a free-field environment, the ratio between the pressure and particle motion is unpredictable for a confined tank environment (Rogers et al., 2016). This is because the pressure to particle

motion ratio changes with distance from the sound source, the water surface, the tank walls and the dimensions and material of the tank itself. Because sharks are sensitive to particle motion, their hearing thresholds would also depend on the acoustic impedance of the test environment. Therefore, the acoustic impedance of the experimental tank was determined at the location of the shark's inner ear at three relevant sound pressure levels (120, 135, and 140 dB re: 1 µPa SPL_{rms}) for all frequencies examined. A hydrophone (TC4013, sensitivity -211 dB re 1 $V\mu Pa^{-1}$; Teledyne Reson Ltd, Slangerup, Denmark) and a waterproofed, neutrally buoyant, triaxial accelerometer (DeltaTron®, Type 4524, National Instruments, Austin, TX, USA; sensitivities: x = 9.770 mV/ms^{-2}, y = 9.977 mV/ms^{-2}, z = 10.02 mV/ms^{-2}) were placed inside the empty animal holder and held in place by rubber bands in the same location as the shark's inner ear. Data from the accelerometer were amplified by a Brüel & Kjær signal conditioning amplifier (NEXUS Type 2690-OS4, Nærum, Denmark) and data from the hydrophone were filtered (HP: 50 Hz, LP: 1 kHz) and amplified by a charge amplifier (VP2000, Teledyne Reson Ltd, Slangerup, Denmark). The peak-to-peak voltage (V_{pk-pk}) for both the pressure wave and the particle acceleration wave of the x-axis (along-body axis, head to tail) were measured on an oscilloscope (Tektronix DPO 2014). The x-axis was chosen because the acoustic power was higher along this axis than along the y (left-right) and z-axis (vertical), due to the position of the speaker 55 cm in front of the shark. Particle acceleration was transformed into particle velocity using the formula $v = a/2\pi f$ (Nedelec et al., 2016). Then, the impedance for each frequency was calculated in MRayl, where 1 Rayl = 1 (Pa s) m−1. These values were then compared with the theoretical free-field impedance of seawater with a salinity of 35 ppt and 15°C and represented on a log scale (dB re: 1.5597 MRayl) (Vetter, Seeley, & Sisneros, 2019). The phase of the impedance was estimated by measuring the phase difference ($\Delta\phi$) between the particle acceleration and the sound pressure wave. Based on the assumption that in the acoustic nearfield the phase of the particle velocity waveform leads the phase of the particle acceleration waveform by 90^o the phase of the impedance was then calculated as $\Delta\phi_{p,\,v} = \Delta\phi_{p,\,a} + 90^o$ (Vetter et al., 2019).

Statistical analysis

The distributions of the response variables (pressure and PAL based AEP thresholds) were normal; hence no transformation of the data was needed. However, with only one

individual showing a threshold at 800 Hz, this observation was removed from the analysis, because no comparisons could be made for that frequency.

The test tank was supplied with ambient seawater, and the water temperature ranged from 14.7 to 22.5 °C over the course of the experimental period, depending on the season. Difference in water temperature can affect the latency and amplitude of the AEP response in marine invertebrates (Jézéquel et al., 2021; Mooney et al., 2010) and has been shown to affect AEP thresholds in some fish (Wysocki, Montey, & Popper, 2009). Sex and total length of the animal may potentially affect hearing abilities and to increase over the course of ontogeny in some species of elasmobranchs (Corwin, 1981c; Corwin, 1983; Parmentier et al., 2020; Sauer, Yopak, & Radford, 2022). To test for any effects of water temperature, total length, and sex on AEP thresholds, linear mixed effects analyses were firstly conducted. PAL-based thresholds were fitted against temperature, total length, and sex as the main effects and random intercepts for each shark subject. Data for each species were analysed in separate models and checked for linear and quadratic curve relationships, respectively. There was no association between threshold and temperature (carpet shark, $t(4) = 0.87$, $p = 0.43$; rig shark, $t(3) = 1.35$, $p = 0.27$; school shark, $t(37) = 1.99$, $p = 0.053$), threshold and total length (carpet shark, $t(4) = 0.13$, $p = 0.91$; rig shark, $t(2) = 0.59$, $p = 0.62$; school shark, $t(37) = 0.92$, $p = 0.36$), and threshold and sex (carpet shark, $t(4) = 0.1$, $p = 0.92$; rig shark, $t(2) = -0.05$, $p = 0.97$; school shark, $t(37) = 0.003$, $p = 0.99$) (**Error! Reference source not found.** S1). Therefore, all data could be grouped to increase sample size and power of the analysis.

To compare the two threshold determination methods (visual and statistical) within each species and each frequency a linear mixed-effects analysis was performed (Bates et al., 2015). Pressure and PAL based thresholds were fitted respectively against a factor, termed 'group' as the main effect and random intercepts for each shark subject. The group factor represents all possible combinations of the variables species, frequency, and method, e.g., Carpet.Shark_80Hz_visual, Carpet.Shark_80Hz_statistical, Rig.Shark_80Hz_visual, etc.). This factor was needed for the models to run properly, as there was not enough overlap in the distribution of frequencies, due to the carpet shark not showing any responses at 450, 600 Hz. Post-hoc pairwise comparisons were used to explore differences between threshold means between methods (within each species and each frequency). Only comparisons within the same species and frequency were examined (e.g., Carpet.Shark_80Hz_visual vs.

Carpet.Shark_80Hz_statistical). All between species and "nonsensical" comparisons (e.g., Carpet.Shark_80Hz_visual vs. Rig.Shark_100Hz_statistical) were ignored.

To compare statistically derived thresholds between species within each frequency linear mixed-effects analyses performed, with only taking the data from the statistical method into account. Pressure and PAL based thresholds were fitted against a factor, termed 'group' (representing all possible combinations of the variables species, frequency, e.g., Carpet.Shark_80Hz, Rig.Shark_80Hz, School.Shark_80Hz, etc.) as the main effect and random intercepts for each shark subject. Post-hoc pairwise comparisons were used to explore differences between threshold means between species (within frequencies). Only comparisons between species (within frequency) were examined (e.g., Carpet.Shark_80Hz vs. Rig.Shark_80Hz). All "nonsensical" or within species comparisons (e.g., Carpet.Shark_80Hz vs. Carpet.Shark_100Hz) were ignored.

P-values were adjusted using the FDR-method and all statistical tests were considered significant at $p < 0.05$. All statistical analyses were performed in R (v4.1.1) (R Core Team) using lmer' in 'lme4' and emmeans' (v1.6) packages.

Results

Acoustic characteristics of the experimental tank

Fast Fourier transformation analyses of the presented stimuli waveforms reveal clear spectral peaks at the respective stimulus frequencies (Figure 2). No acoustic energy was contained in any higher-order harmonics, except for 1200 Hz, which was well outside the hearing range of these three animals.

For lower signal levels (e.g., 120 dB re: 1 µPa) the acoustic energy was equally distributed among the three axes, whereas for higher signal levels (e.g., 135 dB re: µPa) the along-body axis (x: 88.5 + 4.4 dB re: 1 μms^{-2}) had the highest accelerations compared with the y- (79.3 + 3.6 dB re: 1 μms^{-2}) and z-axis (83.4 + 2 dB re: 1 μms^{-2}) across all test frequencies (Figure 3). As expected, the impedance values of our test tank were much lower than in a free-field environment (Figure 4a). This means that the particle acceleration levels, associated with any given sound pressure level, were much higher than what would be

expected in the acoustic farfield in an unbound medium. Further, these results also indicate that there were no major resonances in the tank at any of the test frequencies (Figure 4b).

AEP waveform characteristics

The auditory evoked potential (AEP) waveforms of the three shark species were similar in shape and time course and showed a sharp peak at twice the stimulus frequency in the FFT analysis at suprathreshold levels (Figure 5). A typical suprathreshold AEP response consisted of a series of downward and upward peaks superimposed over a slow negative deflection, that was generally followed by a slow positive deflection, as it is typically described for other fishes (Bullock & Corwin, 1979; Corwin et al., 1982; Kenyon et al., 1998).

Comparison between visually and statistically derived AEP thresholds

The shape and slope of visually and statistically determined threshold curves were similar, however the statistically derived thresholds were consistently below the visually derived thresholds. For both the pressure and PAL determined thresholds the statistical estimates were on average ~4 dB re: 1 µPa below the visual estimates (Figure 6, Tables S1-S2).

Comparison of statistically derived AEP thresholds between different species

Detection threshold curves for pressure and PAL are similar in shape and slope within each species, with sensitivity maxima and minima at the same frequencies (Figure 7). Pressure thresholds were similar between the three species (Figure 7a; Table S3). However, PAL thresholds showed that at 150 Hz the rig shark was more sensitive ($p = 0.004$; average at 74.8 + 1.8 dB re: 1 μms^{-2} PAL_{rms}) than the carpet shark (average at 82.8 + 2.5 dB re: 1 μms^{-2} PAL_{rms}), but not the school shark (average at 79.8 + 1.6 dB re: 1 μms^{-2} PAL_{rms}) (Figure 7b; Table S4). All sharks, except one, responded at frequencies from 80 to 300 Hz, while less than half responded at higher frequencies, and only one rig and none of the school sharks responded at 800 Hz in this study (**Error! Reference source not found.**).

The carpet shark showed the narrowest hearing bandwidth (80 - 300 Hz), with the lowest mean threshold observed at 100 Hz (125.5 + 2.5 dB re: 1 μPa SPL_{rms}/ 82.3 + 1.5 dB re: 1 μms^{-2} PAL_{rms}). The rig shark showed the broadest hearing bandwidth (80 - 800 Hz) and was most sensitive to sounds below 300 Hz, with the lowest mean threshold observed at 150 Hz (119.8 + 2.5 dB re: 1 μPa SPL_{rms}/ 74.8 + 1.8 dB re: 1 μms^{-2} PAL_{rms}). Finally, the school shark responded from 80 to 600 Hz and was most sensitive to frequencies below 200 Hz, with lowest mean thresholds observed at 100 Hz (122.4 + 2.6 dB re: 1 μPa SPL_{rms}/ 79.3 + 1.6 dB re: 1 μms^{-2}, PAL_{rms}).

The background SPL_{rms} and PAL_{rms} in the tank (47-1200 Hz) ranged from 81 to 69 dB re: 1 μPa SPL_{rms} and from 65.3 to 52 dB re: 1 μms^{-2}, respectively, and was below the shark detection thresholds determined here.

Discussion

This study provides novel baseline auditory sensitivity data for three ecologically distinct species of sharks, a fish group of which hearing abilities are largely unknown. Auditory evoked potential detection thresholds were quantified in response to pure tone acoustic stimuli from an underwater speaker. It was found that the three sharks were similar in their overall sensitivities but differed with respect to their upper frequency limits. The bottom dwelling carpet shark had the narrowest frequency detection range (80-300 Hz). Bandwidths were broader for the benthopelagic rig shark (80-800 Hz) and school shark (80-600 Hz). These results show that while hearing abilities were restricted to low frequencies, they do vary between species, suggesting that sound likely plays different roles in these species. Further studies comparing the anatomical structures of the inner ears in the three species are needed to determine which morphological adaptations may be responsible for the observed difference in detectable frequency range.

It is difficult to compare AEP thresholds with behaviourally derived thresholds (Hawkins, 1981). The AEP technique requires the fish to be restrained, often by use of anaesthesia, thus provides information on the response properties of the auditory system at the level of the brainstem, but not at the level of the whole animal (Sisneros et al., 2016). Auditory evoked potential thresholds in fish were shown to be above (~10 dB) behavioural thresholds at frequencies below 1 kHz (Ladich & Fay, 2013; Popper et al., 2019). In addition,

absolute hearing thresholds vary greatly between different studies, due to differences in experimental setups and acoustic environments, making quantitative comparisons of threshold levels impossible (Ladich & Wysocki, 2009; Ladich & Fay, 2013). However, AEP threshold curves and behavioural audiograms can be used to estimate the auditory bandwidth of a species (Ladich & Fay, 2013; Vetter et al., 2018).

It is important to note that we were not able to test frequencies below 80 Hz, due to tank acoustics, and speaker limitations. Therefore, it is very likely that the species examined here can detect frequencies well below 80 Hz, as has been shown for other species of sharks. For instance, the horn shark (*Heterodontus francisi*) (Casper & Mann, 2007a), bamboo sharks [*Chiloscyllium plagiosum*, and *C. punctatum* (Casper & Mann, 2007a; Casper & Mann, 2007b)], and the Atlantic sharpnose shark (*Rhizoprionodon terranovae*) (Casper & Mann, 2009) showed AEP responses to frequencies as low as 20 Hz. And the lemon shark (*Negaprion brevirostris*) has been shown to respond to frequencies as low as 10 Hz in behavioural experiments (Nelson, 1967).

The habitat and lifestyle of a species (e.g., motionless on the seafloor versus swimming in midwater) was proposed as a potential determining factor of the upper hearing limit in elasmobranchs (Corwin, 1981a; Mickle & Higgs, 2022). The present study showed that the demersal carpet shark has a low upper frequency limit of 300 Hz, compared to the more active, benthopelagic school and rig sharks that respond at 600 and 800 Hz, respectively. Physiological and behavioural evidence in other benthic sharks, such as the *C. pliagosum*, *H. francisi* (Casper & Mann, 2007a; Kelly & Nelson, 1975), and the cloudy catshark (*Scyliorhinus torazame*) (Ahn et al., 2011) suggest equally low upper frequency limits (max 300 Hz). However, Corwin's (1977, 1981, 1998) habitat-niche hypothesis to predict hearing abilities in elasmobranchs does not apply to all bottom-dwelling species, as some strictly benthic species have been shown to detect frequencies of up to 1 kHz. For instance, AEP measurements in the bottom-dwelling, small spotted catshark (*Scyliorhinus canicula*) showed an upper frequency limit at 600 Hz (Parmentier et al., 2020) and nurse shark (*Ginglymostoma cirratum*) 1000 Hz (Casper & Mann, 2006). Similarly, benthic batoid species have all showed upper frequency limits around 800 to 1000 Hz (Casper et al., 2003; Casper & Mann, 2006; Corwin, 1983; Mickle, Pieniazek, & Higgs, 2020). Habitat and feeding strategies likely contribute to hearing abilities in elasmobranchs, but there may be other factors (e.g., predation risk, reproduction strategies) driving interspecies differences in elasmobranch hearing abilities. We are currently lacking audiometric data for any of the more

basal Squalomorphii sharks, deep-sea, or purely oceanic species as these are very difficult to keep in captivity (Corwin, 1989). Further comparative physiological, behavioural, and anatomical studies in more species representative of different lifestyles and habitats are needed to resolve the ecological drivers for differences in hearing abilities in elasmobranchs.

The bandwidths and peak sensitivities of AEP detection thresholds of the sharks tested here are comparable with teleost species that only detect particle motion (Ladich & Fay, 2013; Popper & Fay, 2011). Examples are: the flatfishes, such as common dab (*Limanda limanda*) and European plaice (*Pleuronectes platessa*), that have narrow hearing ranges (30-250 Hz) with best hearing at or below 110-160 Hz (Chapman & Sand, 1974); the common triple fin (*Forsterygion lapillum*) with peak sensitivity between 100-200 Hz (Radford et al., 2012); the red-mouthed goby (*Gobius cruentatus*) with upper limit at 700 Hz and peak sensitivity at 100-200 Hz (Wysocki et al., 2009), and kawakawa (*Euthynnus affinis*) with upper limit at 800 Hz and peak sensitivity at 500-600 Hz (Iversen, 1969). The low frequency bandwidth observed in the sharks support previous experimental evidence, suggesting sharks only detect particle motion (Banner, 1967; Kelly & Nelson, 1975).

The results of this study must be evaluated with respect to the limitations of the acoustical setup and the measurement approach. Tank acoustics are very complicated, due to complex interactions of the sound with the water-air boundary and the tank walls (Parvulescu, 1964; Rogers et al., 2016). Therefore, the acoustic condition in the test tank experienced by the shark is very different from the natural free-field environment (Gray et al., 2016; Larsen & Radford, 2018; Popper & Hawkins, 2021). A small sound pressure generated within the tank will produce much larger particle motions, than would be the case in the natural environment (Parvulescu, 1964). As a result, the hearing abilities of the sharks may be unnaturally extended to higher frequencies in a tank setting (Chapman & Sand, 1974). Ideally hearing thresholds should be measured in the free field (e.g., Chapman and Sand, 1974; Hawkins and Chapman 1975; Hawkins and Johnstone, 1978). It would be particularly interesting to conduct free field experiments within both the acoustic nearfield and far-field, to solve the currently unanswered question of how far from a sound source sharks can detect sound (Casper & Mann, 2006; Casper & Mann, 2009). In this study, the shark was positioned

within the acoustic nearfield[1], which the impedance results confirm (Vetter et al., 2019). In addition, in the nearfield there exists hydrodynamic flow that is generated by the vibrations of the underwater loudspeaker (Kalmijn, 1988). It has been shown that in some teleost fishes the lateral line responds to these flows up to frequencies of 200 Hz. (Braun & Coombs, 2000; Harris & van Bergeijk, 1962; Higgs & Radford, 2013; Hueter et al., 2004; Maruska & Sisneros, 2016). Therefore, the AEP responses measured at frequencies below 200 Hz may potentially contain contributions from the lateral line system.

Conclusions

In summary, this study assessed AEP sensitivities to acoustic stimuli from an underwater speaker in the benthic New Zealand carpet shark, and the benthopelagic rig, and school shark. The three species have similar sensitivities but differ in their upper frequency limit. Our results indicate that the hearing abilities of the three shark species, were most consistent with those known for hearing 'non-specialists' fishes that only detect the particle motion component of the sound field. Further, our results provide evidence that benthopelagic sharks can hear higher frequencies (max. 800 Hz) than some of the bottom dwelling-sharks (max. 300 Hz). Finally, the AEP detection thresholds presented here likely provide a good first approximation of the basic hearing abilities for the three shark species. However, to test what ecological factors are driving the observed interspecific differences in hearing bandwidth further behavioural and morphological studies are needed.

Acknowledgements

The authors would like to thank Errol Murray, Gavin Perry, Derek Sauer, Stefan Spreitzenbarth, and Stefano Schoene from the Leigh Marine Lab for their help with the animal collections. We would like to express our gratitude to Jenni Stanley and Paul Caiger for their help troubleshooting the AEP setup. We are grateful to Jessica McLay for help with

[1] Assuming the boundary of the acoustic nearfield for a monopole source is approximately equal to $\lambda/2\pi$ (Yan, Anraku, & Babaran, 2010).

statistics. This project was funded by the Marsden grant# UOA1808 to Craig Radford and by the University of Auckland Doctoral Scholarship to Carolin Nieder.

References

Backus, R. H. (1963). Hearing in elasmobranchs. In G. W. Perry (Ed.), *Sharks and survival* (pp. 243-254). D. C. Heath and Company, Boston, MA, USA.

Banner, A. (1967). Evidence of sensitivity to acoustic displacements in the lemon shark, *Negaprion brevirostris* (Poey). In P. Cahn (Ed.), *Lateral line detectors* (pp. 265-273). New York, NY (USA): Indiana University Press.

Banner, A. (1972). Use of sound in predation by young lemon sharks, *Negaprion brevirostris* (Poey). *Bulletin of Marine Science, 22*(2), 251-283.

Bates, D., Mächler, M., Bolker, B., & Walker, S. (2015). Fitting linear mixed-effects models using lme4. *Journal of Statistical Software, 67*(1), 1-48. doi:10.18637/jss.v067.i01

Braun, C. B., & Coombs, S. (2000). The overlapping roles of the inner ear and lateral line: The active space of dipole source detection. *Philosophical Transactions of the Royal Society of London. Series B: Biological Sciences, 355*(1401), 1115-1119. doi:10.1098/rstb.2000.0650

Bullock, T. H., & Corwin, J. T. (1979). Acoustic evoked activity in the brain in sharks. *Journal of Comparative Physiology A, 129*(3), 223-234. doi:10.1007/BF00657658

Carrier, J. C., Pratt, H. L., & Martin, L. K. (1994). Group reproductive behaviors in free-living nurse sharks, *Ginglymostoma cirratum*. *Copeia, 1994*(3), 646-656. doi:10.2307/1447180

Casper, B. M., Lobel, P. S., & Yan, H. Y. (2003). The hearing sensitivity of the little skate, *Raja erinacea*: A comparison of two methods. *Environmental Biology of Fishes, 68*(4), 371-379. doi:10.1023/B:EBFI.0000005750.93268.e4

Casper, B. M., & Mann, D. A. (2006). Evoked potential audiograms of the nurse shark (*Ginglymostoma cirratum*) and the yellow stingray (*Urobatis jamaicensis*). *Environmental Biology of Fishes, 76*(1), 101-108. doi:10.1007/s10641-006-9012-9

Casper, B. M., & Mann, D. A. (2007a). Dipole hearing measurements in elasmobranch fishes. *Journal of Experimental Biology, 210*(1), 75-81. doi:10.1242/jeb.02617

Casper, B. M., & Mann, D. A. (2007b). The directional hearing abilities of two species of bamboo sharks. *Journal of Experimental Biology, 210*(3), 505-511. doi:10.1242/jeb.02677

Casper, B. M., & Mann, D. A. (2009). Field hearing measurements of the Atlantic sharpnose shark *Rhizoprionodon terraenovae*. *Journal of Fish Biology, 75*(10), 2768-2776. doi:10.1111/j.1095-8649.2009.02477.x

Chapman, C., & Sand, O. (1974). Field studies of hearing in two species of flatfish *Pleuronectes platessa* (L.) and *Limanda limanda* (L.) (Family Pleuronectidae). *Comparative Biochemistry and Physiology Part A: Physiology, 47*(1), 371-385. doi:10.1016/0300-9629(74)90082-6

Chapuis, L., & Collin, S. P. (2022). The auditory system of cartilaginous fishes. *Reviews in Fish Biology and Fisheries, 32*(72), 521–554. doi:10.1007/s11160-022-09698-8

Chapuis, L., Collin, S. P., Yopak, K. E., McCauley, R. D., Kempster, R. M., Ryan, L. A., . . . Egeberg, C. A. (2019). The effect of underwater sounds on shark behaviour. *Scientific Reports, 9*(1), 1-11. doi:10.1038/s41598-019-43078-w

Christensen, C. B., Christensen-Dalsgaard, J., & Madsen, P. T. (2015). Hearing of the African lungfish (*Protopterus annectens*) suggests underwater pressure detection and rudimentary aerial hearing in early tetrapods. *Journal of Experimental Biology, 218*(3), 381-387. doi:10.1242/jeb.116012

Corwin, J. T. (1977). Morphology of the macula neglecta in sharks of the genus *Carcharhinus*. *Journal of Morphology, 152*(3), 341-361. doi:10.1002/jmor.1051520306

Corwin, J. T. (1978). The relation of inner ear structure to the feeding behavior in sharks and rays. In O. Johari (Ed.), *Scanning electron microscopy* (pp. 1105-1112) S.E.M. Inc.

Corwin, J. T. (1981a). Audition in elasmobranchs. In W. N. Tavolga, A. N. Popper & R. R. Fay (Eds.), *Hearing and sound communication in fishes* (pp. 81-105) Springer. doi:10.1007/978-1-4615-7186-5_5

Corwin, J. T. (1981b). Peripheral auditory physiology in the lemon shark: Evidence of parallel otolithic and non-otolithic sound detection. *Journal of Comparative Physiology, 142*(3), 379-390. doi:10.1007/BF00605450

Corwin, J. T. (1981c). Postembryonic production and aging of inner ear hair cells in sharks. *Journal of Comparative Neurology, 201*(4), 541-553. doi:10.1002/cne.902010406

Corwin, J. T. (1983). Postembryonic growth of the macula neglecta auditory detector in the ray, *Raja clavata*: Continual increases in hair cell number, neural convergence, and physiological sensitivity. *Journal of Comparative Neurology, 217*(3), 345-356. doi:10.1002/cne.902170309

Corwin, J. T. (1989). Functional anatomy of the auditory system in sharks and rays. *Journal of Experimental Zoology, 252*(S2), 62-74. doi:10.1002/jez.1402520408

Corwin, J. T., Bullock, T. H., & Schweitzer, J. (1982). The auditory brain stem response in five vertebrate classes. *Electroencephalography and Clinical Neurophysiology, 54*(6), 629-641. doi:10.1016/0013-4694(82)90117-1

Dinh, J. P., & Radford, C. A. (2021). Acoustic particle motion detection in the snapping shrimp (*Alpheus richardsoni*). *Journal of Comparative Physiology A, 207*(5), 641-655. doi:10.1007/s00359-021-01503-4

Ebert, D. A., Dando, M., & Fowler, S. (2021). *A pocket guide to sharks of the world* Princeton University Press. doi:10.2307/j.ctv1cmsmwn

Fay, R. R. (1974). Sound reception and processing in the carp: Saccular potentials. *Comparative Biochemistry and Physiology Part A: Physiology, 49*(1), 29-42. doi:10.1016/0300-9629(74)90539-8

Fay, R. R., Kendall, J. I., Popper, A. N., & Tester, A. L. (1974). Vibration detection by the macula neglecta of sharks. *Comparative Biochemistry and Physiology Part A: Physiology, 47*(4), 1235-1240. doi:10.1016/0300-9629(74)90097-8

Fay, R. R., & Popper, A. N. (2000). Evolution of hearing in vertebrates: the inner ears and processing. *Hearing Research, 149*(1-2), 1-10. doi:10.1016/S0378-5955(00)00168-4

Fetterplace, L. C., Esteban, J. D., Pini-Fitzsimmons, J., Gaskell, J., & Wueringer, B. E. (2022). Evidence of sound production in wild stingrays. *Ecological Society of America, 103*, e3812. doi:10.1002/ecy.3812

Flock, A. (1971). Sensory transduction in hair cells. In W. Loewenstein (Ed.), *Principles of receptor physiology* (pp. 396-441) Springer. doi:10.1007/978-3-642-65063-5_14

Flock, A., & Wersall, J. (1963). Morphological polarization and orientation of hair cells in labyrinth and lateral line organ. *Journal of Ultrastructure Research, 8*(1), 193-194.

Francis, M. P., & Francis, R. (1992). Growth rate estimates for New Zealand rig (*Mustelus lenticulatus*). *Marine and Freshwater Research, 43*(5), 1157-1176. doi:10.1071/MF9921157

Francis, M. P., Lyon, W., Jones, E., Notman, P., Parkinson, D., & Getzlaff, C. (2012). *Rig nursery grounds in New Zealand: A review and survey. New Zealand Aquatic Environment and Biodiversity Report.* (No. 95).

Francis, M. P., & Mulligan, K. P. (1998). Age and growth of New Zealand school shark, *Galeorhinus galeus*. *New Zealand Journal of Marine and Freshwater Research, 32*(3), 427-440. doi:10.1080/00288330.1998.9516835

Gray, M. D., Rogers, P. H., Popper, A. N., Hawkins, A. D., & Fay, R. R. (2016). "Large" tank acoustics: How big is big enough? In A. N. Popper, & A. D. Hawkins (Eds.), *The effects of noise on aquatic life II* (pp. 363-369) Springer. doi:10.1007/978-1-4939-2981-8_43

Harris, G. G., & van Bergeijk, W. A. (1962). Evidence that the lateral-line organ responds to near-field displacements of sound sources in water. *The Journal of the Acoustical Society of America, 34*(12), 1831-1841. doi:10.1121/1.1909138

Hawkins, A. D. (1981). The hearing abilities of fish. In W. N. Tavolga, A. N. Popper & R. R. Fay (Eds.), *Hearing and sound communication in fishes* (pp. 109-137) Springer. doi:10.1007/978-1-4615-7186-5_6

Higgs, D. M., & Radford, C. A. (2013). The contribution of the lateral line to 'hearing' in fish. *Journal of Experimental Biology, 216*(8), 1484-1490. doi:10.1242/jeb.078816

Horn, P. L. (2016). Biology of the New Zealand carpet shark *Cephaloscyllium isabellum* (Scyliorhinidae). *Journal of Ichthyology, 56*(3), 336-347. doi:10.1134/S0032945216030048

Hueter, R. E., Mann, D. A., Maruska, K. P., Sisneros, J. A., & Demski, L. S. (2004). Sensory biology of elasmobranchs. In P. L. Lutz (Ed.), *Biology of sharks and their relatives* (pp. 325-368) CRC Press; Taylor & Francis Group.

Iversen, R. (1969). *Auditory thresholds of the scombrid fish (Euthynnus affinis) with comments on the use of sound in tuna fishing. Fisheries and Aquaculture Report (FAO).* (No. 62).FAO.

Jézéquel, Y., Jones, I. T., Bonnel, J., Chauvaud, L., Atema, J., & Mooney, A. T. (2021). Sound detection by the American lobster (*Homarus americanus*). *Journal of Experimental Biology*, *224*(6), jeb240747. doi:10.1242/jeb.240747

Kalmijn, A. J. (1988). Hydrodynamic and acoustic field detection. In J. Atema, R. R. Fay, A. N. Popper & W. N. Tavolga (Eds.), *Sensory biology of aquatic animals* (pp. 83-130) Springer. doi:10.1007/978-1-4612-3714-3_4

Kelly, J. C., & Nelson, D. R. (1975). Hearing thresholds of the horn shark, *Heterodontus francisci*. *The Journal of the Acoustical Society of America*, *58*(4), 905-909. doi:10.1121/1.380742

Kenyon, T. N., Ladich, F., & Yan, H. Y. (1998). A comparative study of hearing ability in fishes: The auditory brainstem response approach. *Journal of Comparative Physiology A*, *182*(3), 307-318. doi:10.1007/s003590050181

Klimley, P., & Myrberg, A. A. (1979). Acoustic stimuli underlying withdrawal from a sound source by adult lemon sharks, *Negaprion Brevirostris* (Poey). *Bulletin of Marine Science*, *29*(4), 447-458.

Ladich, F., & Fay, R. R. (2013). Auditory evoked potential audiometry in fish. *Reviews in Fish Biology and Fisheries*, *23*(3), 317-364. doi:10.1007/s11160-012-9297-z

Ladich, F., & Wysocki, L. E. (2009). Does speaker presentation affect auditory evoked potential thresholds in goldfish? *Comparative Biochemistry and Physiology Part A: Molecular & Integrative Physiology*, *154*(3), 341-346. doi:10.1016/j.cbpa.2009.07.004

Larsen, O. N., & Radford, C. (2018). Acoustic conditions affecting sound communication in air and underwater. In H. Slabbekoorn, R. J. Dooling, A. N. Popper & R. R. Fay (Eds.), *Effects of anthropogenic noise on animals* (pp. 109-144) Springer. doi:10.1007/978-1-4939-8574-6_5

Lauridsen, T. B., Brandt, C., & Christensen-Dalsgaard, J. (2021). Three auditory brainstem response (ABR) methods tested and compared in two anuran species. *Journal of Experimental Biology*, *224*(2), jeb237313. doi:10.1242/jeb.237313

Lowenstein, O. E. (1971). The Labyrinth. In W. Hoar, & D. Randall (Eds.), *Fish physiology* (pp. 207-240). New York and London: Elsevier. doi:10.1016/S1546-5098(08)60048-5

Lowenstein, O. E., & Roberts, T. (1950). The equilibrium function of the otolith organs of the thornback ray (*Raja clavata*). *The Journal of Physiology*, *110*(3-4) doi:10.1113/jphysiol.1949.sp004448

Lowenstein, O. E., & Roberts, T. (1951). The localization and analysis of the responses to vibration from the isolated elasmobranch labyrinth. A contribution to the problem of the evolution of hearing in vertebrates. *The Journal of Physiology, 114*(4), 471-489. doi:10.1113/jphysiol.1951.sp004638

Maisey, J. G., & Lane, J. A. (2010). Labyrinth morphology and the evolution of low-frequency phonoreception in elasmobranchs. *Comptes Rendus Palevol, 9*(6-7), 289-309. doi:10.1016/j.crpv.2010.07.021

Maruska, K. P., & Sisneros, J. A. (2016). Comparison of electrophysiological auditory measures in fishes. In J. A. Sisneros (Ed.), *Fish hearing and bioacoustics* (pp. 227-254) Springer. doi:10.1007/978-3-319-21059-9_11

Mickle, M. F., & Higgs, D. M. (2022). Towards a new understanding of elasmobranch hearing. *Marine Biology, 169*(1), 1-13. doi:10.1007/s00227-021-03996-8

Mickle, M. F., Pieniazek, R. H., & Higgs, D. M. (2020). Field assessment of behavioural responses of southern stingrays (*Hypanus americanus*) to acoustic stimuli. *Royal Society Open Science, 7*(1), 191544. doi:10.1098/rsos.191544

Mooney, A. T., Hanlon, R. T., Christensen-Dalsgaard, J., Madsen, P. T., Ketten, D. R., & Nachtigall, P. E. (2010). Sound detection by the longfin squid (*Loligo pealeii*) studied with auditory evoked potentials: Sensitivity to low-frequency particle motion and not pressure. *Journal of Experimental Biology, 213*(21), 3748-3759. doi:10.1242/jeb.048348

Mulligan, K. P., & Gauldie, R. (1989). The biological significance of the variation in crystalline morph and habit of otoconia in elasmobranchs. *Copeia, 4*, 856-871. doi:10.2307/1445969

Myrberg, A. A. (1972). Using sound to influence the behaviour of free-ranging marine animals. In H. E. Winn, & B. L. Olla (Eds.), *Behavior of marine animals. Current perspectives in research volume 2: Vertebrates* (pp. 435-468) Springer. doi:10.1007/978-1-4684-0910-9_7

Myrberg, A. A., Gordon, C. R., & Klimley, P. (1976). Attraction of free ranging sharks by low frequency sound, with comments on its biological significance. In A. Schuijf, & A. D. Hawkins (Eds.), *Sound reception in fish* (pp. 205-228). Amsterdam: Elsevier. doi:256932252

Myrberg, A. A., Gordon, C. R., & Klimley, P. (1978). Rapid withdrawal from a sound source by open-ocean sharks. *The Journal of the Acoustical Society of America, 64*(5), 1289-1297. doi:10.1121/1.382114

Nachtigall, P. E., Mooney, A. T., Taylor, K. A., & Yuen, M. M. (2007). Hearing and auditory evoked potential methods applied to odontocete cetaceans. *Aquatic Mammals, 33*(1), 6. doi:10.1578/AM.33.1.2007.6

Nachtigall, P. E., Supin, A. Y., Pawloski, J., & Au, W. W. (2004). Temporary threshold shifts after noise exposure in the bottlenose dolphin (*Tursiops truncatus*) measured using evoked auditory potentials. *Marine Mammal Science, 20*(4), 673-687. doi:10.1111/j.1748-7692.2004.tb01187.x

Nedelec, S. L., Campbell, J., Radford, A. N., Simpson, S. D., & Merchant, N. D. (2016). Particle motion: The missing link in underwater acoustic ecology. *Methods in Ecology and Evolution, 7*(7), 836-842. doi:10.1111/2041-210X.12544

Nelson, D. R. (1967). Hearing thresholds, frequency discrimination, and acoustic orientation in the lemon shark, *Negaprion brevirostris* (Poey). *Bulletin of Marine Science, 17*(3), 741-768.

Nelson, D. R., & Gruber, S. H. (1963). Sharks: Attraction by low-frequency sounds. *Science, 142*(3594), 975-977. doi:10.1126/science.142.3594.97

Nelson, D. R., & Johnson, R. H. (1970). *Acoustic studies on sharks, Rangiroa Atoll, July, 1969.* (No. Technical Report No. AD0709104).

Parmentier, E., Banse, M., Boistel, R., Compère, P., Bertucci, F., & Colleye, O. (2020). The development of hearing abilities in the shark *Scyliorhinus canicula*. *Journal of Anatomy, 237*(3), 468-477. doi:10.1111/joa.13212

Parvulescu, A. (1964). Problems of propagation and processing. In W. N. Tavolga (Ed.), *Marine bioacoustics* (pp. 87-100) Pergamon Press.

Popper, A. N., & Fay, R. R. (1977). Structure and function of the elasmobranch auditory system. *American Zoologist, 17*(2), 443-452. doi:10.1093/icb/17.2.443

Popper, A. N., & Fay, R. R. (2011). Rethinking sound detection by fishes. *Hearing Research, 273*(1-2), 25-36. doi:10.1016/j.heares.2009.12.023

Popper, A. N., & Hawkins, A. D. (2021). Fish hearing and how it is best determined. *ICES Journal of Marine Science, 78*(7), 2325-2336. doi:10.1093/icesjms/fsab115

Popper, A. N., Hawkins, A. D., Sand, O., & Sisneros, J. A. (2019). Examining the hearing abilities of fishes. *The Journal of the Acoustical Society of America, 146*(2), 948-955. doi:10.1121/1.5120185

Popper, A. N., Hawkins, A. D., & Sisneros, J. A. (2021). Fish hearing "Specialization"–A re-evaluation. *Hearing Research, 425*, 108393. doi:10.1016/j.heares.2021.108393

Radford, C. A., Montgomery, J. C., Caiger, P., & Higgs, D. (2012). Pressure and particle motion detection thresholds in fish: A re-examination of salient auditory cues in teleosts. *The Journal of Experimental Biology, 215*(Pt 19), 3429-3435. doi:10.1242/jeb.073320

Retzius, G. (1881). *Das Gehörorgan der Fische und Amphibien* Samson & Wallin.

Richard, J. D. (1968). Fish attraction with pulsed low-frequency sound. *Journal of the Fisheries Board of Canada, 25*(7), 1441-1452. doi:10.1139/f68-125

Rogers, P. H., & Cox, M. (1988). Underwater sound as a biological stimulus. In J. Atema, R. R. Fay, A. N. Popper & W. N. Tavolga (Eds.), *Sensory biology of aquatic animals* (pp. 131-149) Springer. doi:10.1007/978-1-4612-3714-3_5

Rogers, P. H., Hawkins, A. D., Popper, A. N., Fay, R. R., & Gray, M. D. (2016). Parvulescu revisited: Small tank acoustics for bioacousticians. In A. N. Popper, & A. Hawkins

(Eds.), *The effects of noise on aquatic life II* (pp. 933-941) Springer. doi:10.1007/978-1-4939-2981-8_115

Sand, O., & Enger, P. S. (1973). Evidence for an auditory function of the swimbladder in the cod. *Journal of Experimental Biology, 59*(2), 405-414. doi:10.1242/jeb.59.2.405

Sauer, D. J., Yopak, K. E., & Radford, C. A. (2022). Ontogeny of the inner ear maculae in school sharks (*Galeorhinus galeus*). *Hearing Research, 424*, 108600. doi:10.1016/j.heares.2022.108600

Sisneros, J. A., Popper, A. N., Hawkins, A. D., & Fay, R. R. (2016). Auditory evoked potential audiograms compared with behavioral audiograms in aquatic animals. In A. N. Popper, & A. D. Hawkins (Eds.), *The effects of noise on aquatic life II* (pp. 1049-1056) Springer. doi:10.1007/978-1-4939-2981-8_130

Tester, A. L., Kendall, J. I., & Milisen, W. B. (1972). Morphology of the ear of the shark genus *Carcharhinus*, with particular reference to the macula neglecta. *Pacific Science, 26*(3), 264-274. doi:10.1002/jmor.1051520306

Vetter, B. J., Brey, M. K., & Mensinger, A. F. (2018). Reexamining the frequency range of hearing in silver (*Hypophthalmichthys molitrix*) and bighead (*H. nobilis*) carp. *PLoS One, 13*(3), e0192561. doi:10.1371/journal.pone.0192561

Vetter, B. J., Seeley, L. H., & Sisneros, J. A. (2019). Lagenar potentials of the vocal plainfin midshipman fish, *Porichthys notatus*. *Journal of Comparative Physiology A, 205*(1), 163-175. doi:10.1007/s00359-018-01314-0

Wiernicki, C. J., Liang, D., Bailey, H., & Secor, D. H. (2020). The effect of swim bladder presence and morphology on sound frequency detection for fishes. *Reviews in Fisheries Science & Aquaculture, 28*(4), 459-477. doi:10.1080/23308249.2020.1762536

Wysocki, L. E., Codarin, A., Ladich, F., & Picciulin, M. (2009). Sound pressure and particle acceleration audiograms in three marine fish species from the Adriatic Sea. *The Journal of the Acoustical Society of America, 126*(4), 2100-2107.

Wysocki, L. E., Montey, K., & Popper, A. N. (2009). The influence of ambient temperature and thermal acclimation on hearing in a eurythermal and a stenothermal otophysan fish. *Journal of Experimental Biology, 212*(19), 3091-3099. doi:10.1242/jeb.033274

Xiao, J., & Braun, C. B. (2008). Objective threshold estimation and measurement of the residual background noise in auditory evoked potentials of goldfish. *The Journal of the Acoustical Society of America, 124*(5), 3053-3063. doi:10.1121/1.2982366

Yan, H. Y., Anraku, K., & Babaran, R. P. (2010). Hearing in marine fish and its application in fisheries. In P. He (Ed.), *Behavior of marine fishes: Capture processes and conservation challenges* (pp. 45-64) Wiley-Blackwell. doi:10.1002/9780813810966.ch3

Figures and Tables

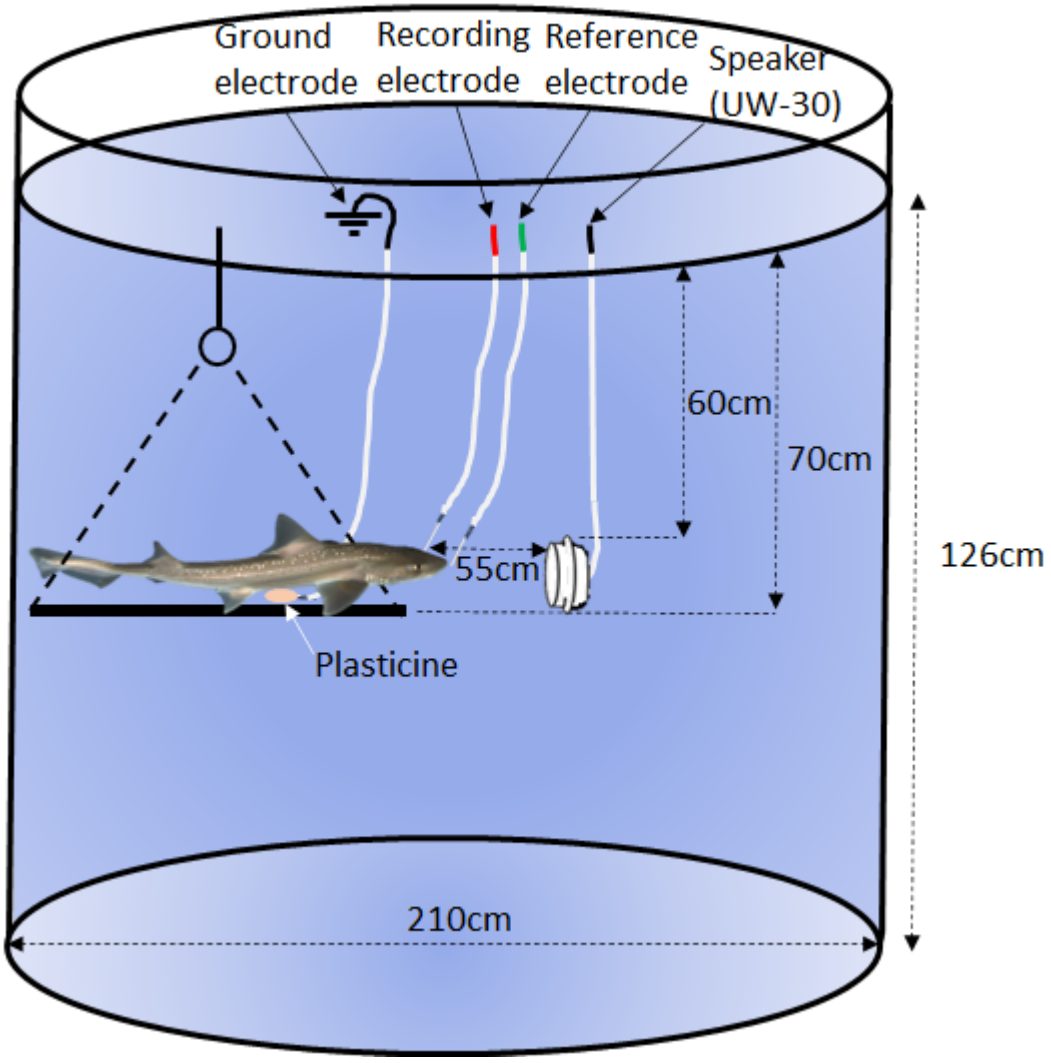

Fig. 1. Experimental tank setup. The shark was attached to a custom-made plastic mesh holder (not shown) and suspended ~70 cm below the waterline, such that the inner ear of the shark was positioned 55 cm in front and 5 cm above the underwater loudspeaker. The recording electrode (red) was inserted dorsally, underneath the skin, at the border of the parietal fossa, where it has its widest (medial-lateral) diameter. The reference electrode (green) was inserted into the cartilage at the tip of the snout, and the ground electrode (black) was placed in plasticine next to the shark's body. The underwater speaker and electrode wires were wrapped in tinfoil and grounded to shield from electrical noise.

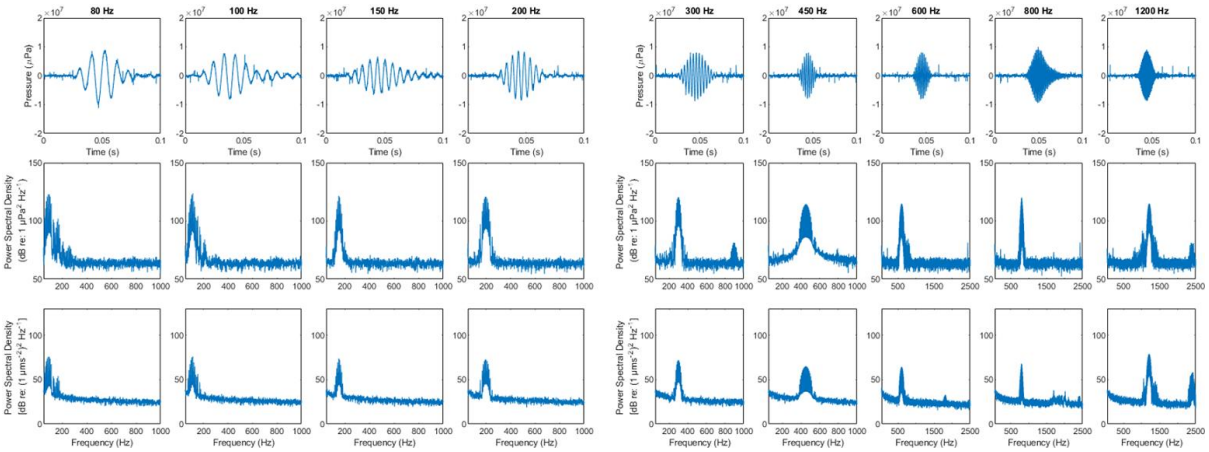

Fig. 2. Representative examples of the stimulus waveforms for test frequencies 80 - 1200 Hz. The corresponding power spectra are plotted for shown below each waveform in both pressure (dB re: 1 μPa^2 Hz^{-1}) and particle acceleration [dB re: (1 μm s^{-2})^2 Hz^{-1}]. All tone-bursts are shown at a sound pressure level of 135 dB re: 1 μPa. Measurements were made using a hydrophone and a triaxial accelerometer in the same place, where the shark's inner ear was positioned.

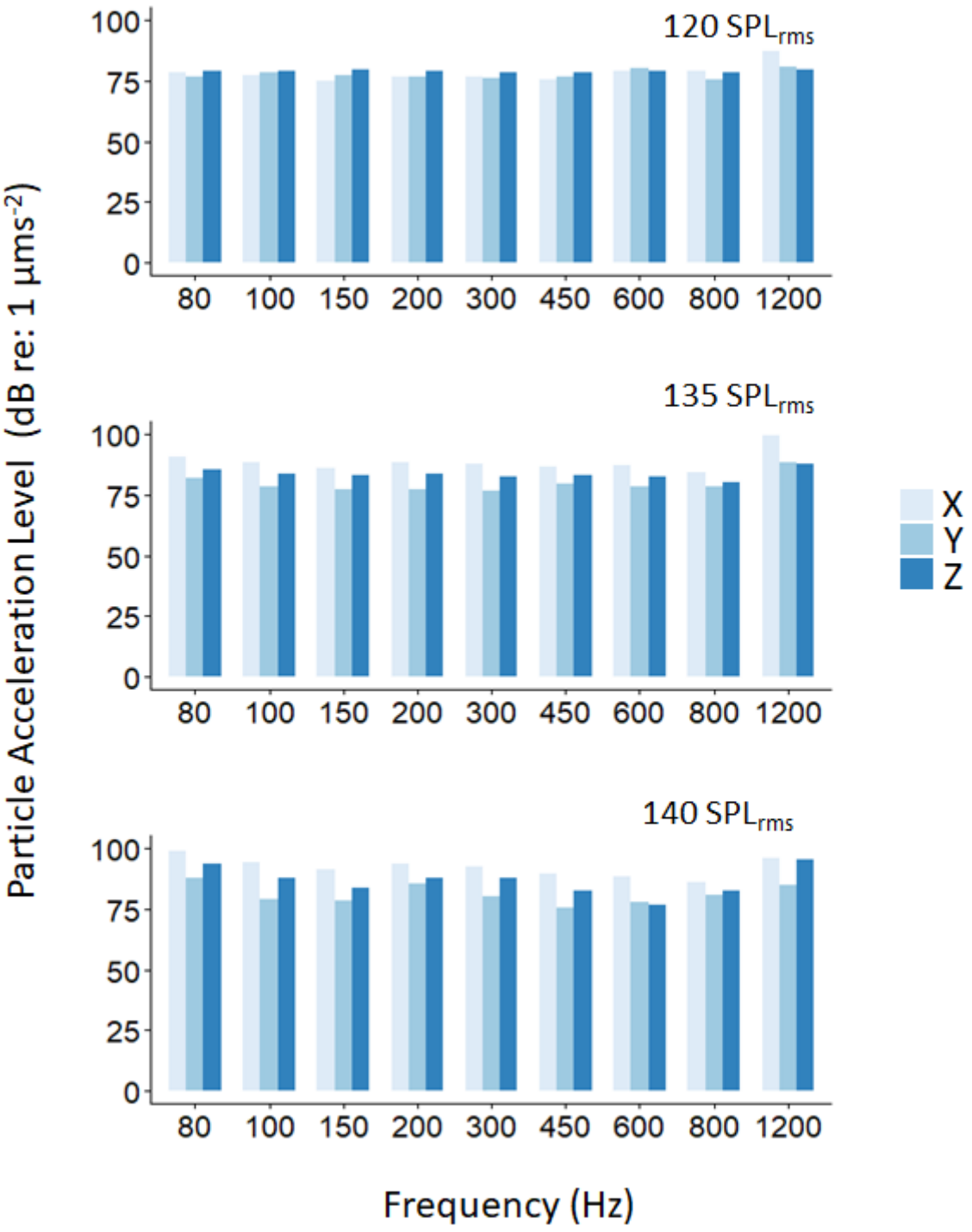

Fig. 3. Speaker generated particle acceleration levels (dB re: 1 µm-2 PAL_{rms}) in all three dimensions. [X-axis (anterior-posterior) = light blue, y-axis (medial-lateral) = medium blue, z-axis (vertical) = dark blue] at all frequencies examined for three sound pressure levels (SPL_{rms}): 120, 135, and 140 dB re: 1 µPa. Measurements were made using a triaxial accelerometer in the same place, where the shark's inner ear was positioned.

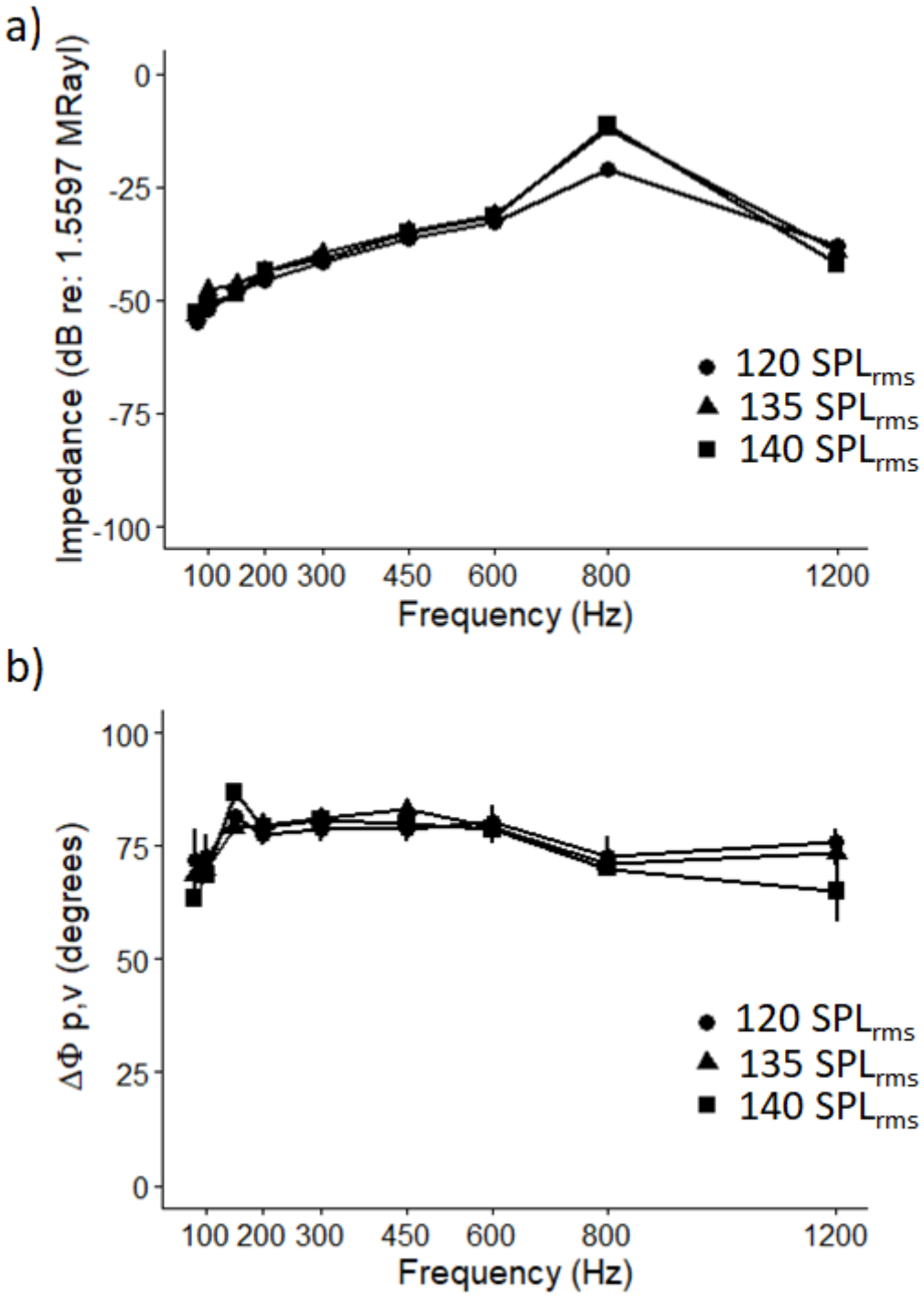

Fig. 4. Acoustic characteristics of the experimental tank and speaker. (a) Acoustic impedance [Z = ratio of sound pressure (Pa) to particle velocity (ms^{-1}) in x-direction] relative to 1.5597 MRayl (the reference impedance for a free-field in 35 ppt salinity seawater at 15^{o}C) plotted for all the frequencies examined at three sound pressure levels (SPL_{rms}) 120, 135, and 140 dB re: 1µPa. (b) Phase differences (Δ) between the pressure and particle velocity waves.

Measurements (n= 3 for each frequency and SPL) were made using a hydrophone and a triaxial accelerometer placed in the same place, where the shark's inner ear was positioned. All data are plotted as the mean (+ 1 SD).

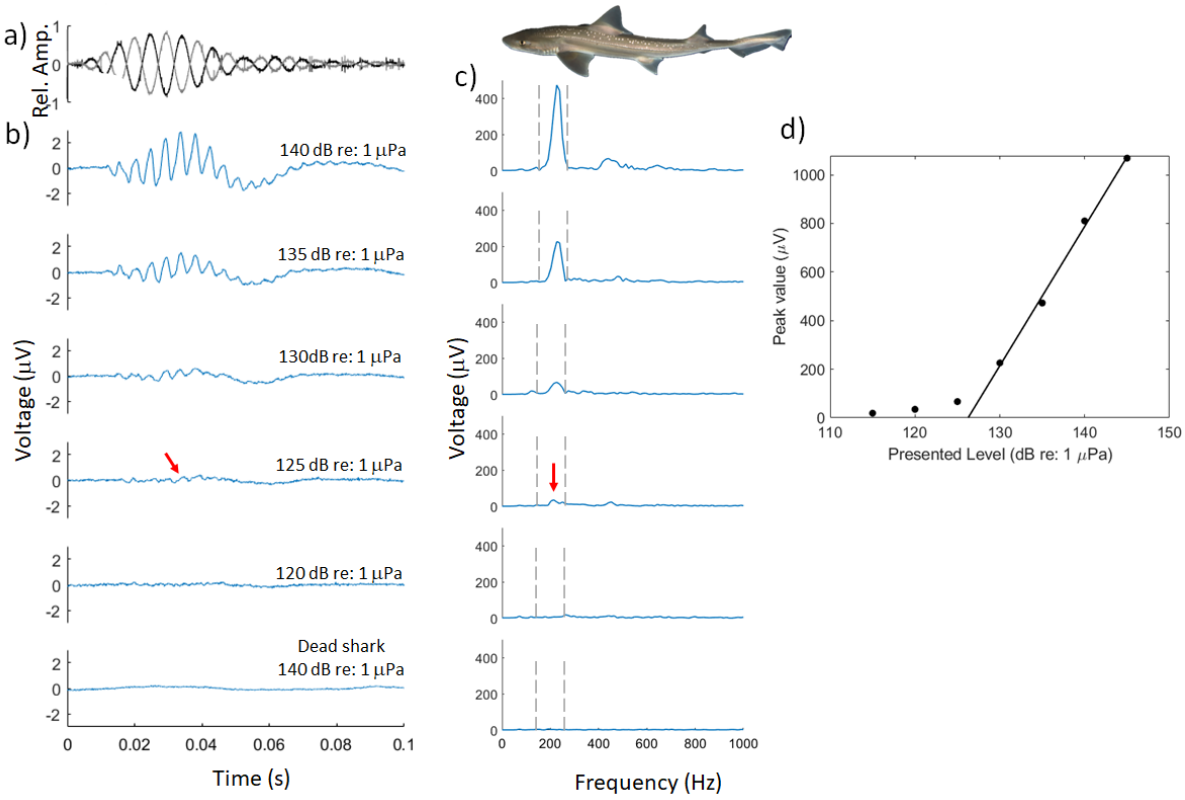

Fig. 5. Characteristic examples of speaker generated AEP waveforms with corresponding FFT-spectra, and threshold determination procedures shown for a rig shark (*Mustelus lenticulatus*). (a) Examples shown for a 100 Hz Hann-gated acceleration signal (50 ms) presented at opposing polarities of 0^{o} (black) and 180^{o} (grey). (b) Average AEP waveforms were collected for signal levels ranging from 145 to 120 dB re 1 µPa SPL_{rms} in decreasing steps of 5 dB. Each response was collected using 1200 sweep averages (600 at a stimulus polarity of 0^{o} and 600 at 180^{o}). The red arrow highlights the lowest visually distinguishable responses at 125 dB re: 1 µPa SPL_{rms}. The last trace shows the control test where the active electrode was in the standard recording position, but the animal was dead. (c) Corresponding 2048-point FFTs of the entire 100 ms duration of the traces. The peak frequency of the observed responses was twice the frequency of the 100 Hz tone-pip stimulus (200 Hz shown by the red arrow). The maximum FFT value was found across the five FFT bins greater than and five FFT bins less than twice the presented frequency (143-262 Hz) as delineated by the dotted grey lines. (d) For statistical threshold determination the maximum FFT voltage (peak value) between these frequency bins was plotted against the presented sound pressure level, and the x-intercept of the best fitting regression line was used as estimate of the animal's AEP threshold. The statistically derived AEP thresholds at 100 Hz for this individual was 126.26 dB re: 1 µPa SPL_{rms}.

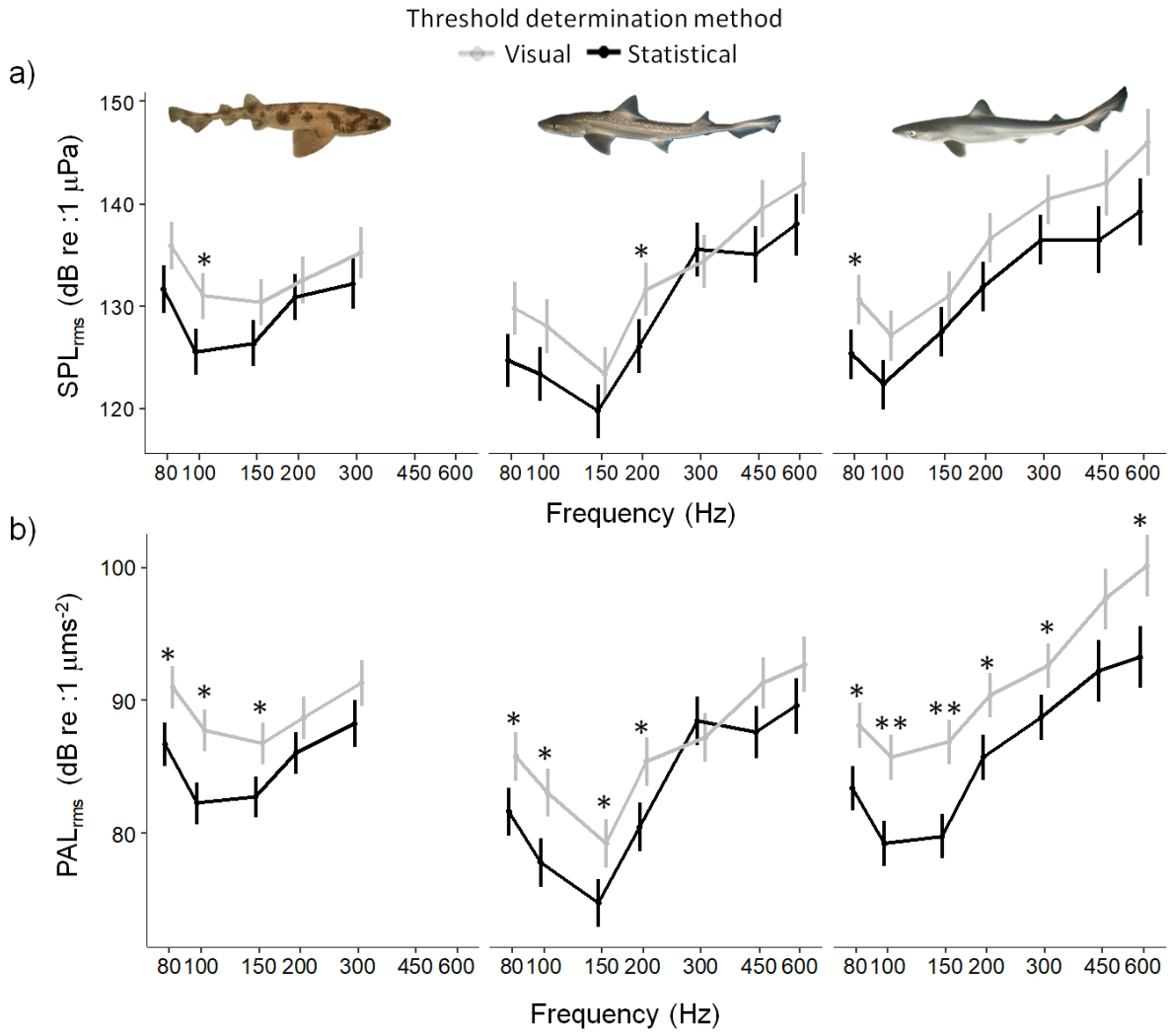

Fig. 6. Comparison of visual and statistical (objective) threshold determination methods. Visually (grey) and statistically (black) derived AEP threshold curves are shown for the carpet shark (*Cephaloscyllium isabellum*), rig shark (*Mustelus lenticulatus*), and school shark (*Galeorhinus galeus*). Thresholds are shown based on (a) sound pressure level (dB re: 1 µPa SPL_{rms}) and (b) particle acceleration level (dB re: 1 µms^{-2} PAL_{rms}). All data shown as mean (+1 s.e.m.). The stars (*) indicate the results of post-hoc pairwise comparisons between methods, within each species and frequency. Means that were not significantly different by the Tukey-test at the 5% level of significance do not have a star. Legend: **, $p < 0.001$; *, $p < 0.05$.

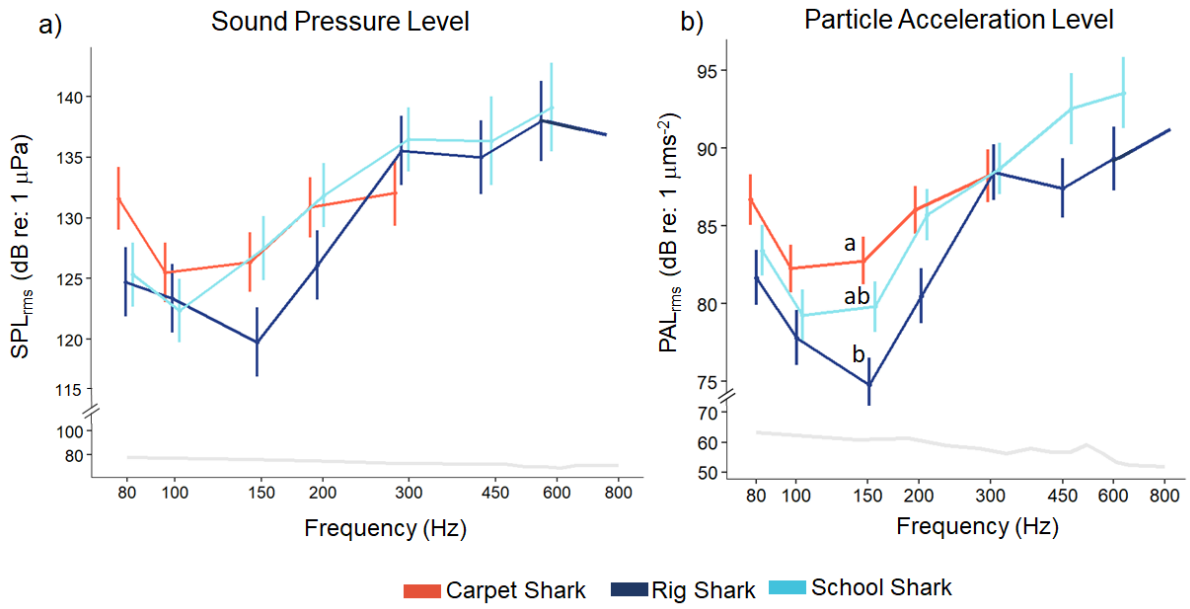

Fig. 7. AEP sensitivities for the carpet shark (*Cephaloscyllium isabellum*), rig shark (*Mustelus lenticulatus*), and school shark (*Galeorhinus galeus*) measured in a tank and underwater speaker setup. Thresholds were determined statistically using the x-intercept method and are shown as mean (+1 s.e.m.) in terms of (a) sound pressure level (dB re: 1 µPa SPL_{rms}) and (b) particle acceleration level (dB re: 1 µms^{-2} PAL_{rms}). Grey lines indicate ambient sound levels. Lowercase letters indicate results of post-hoc pairwise comparisons between species, within each frequency. Means not sharing any common letter are significantly different by the Tukey-test at the 5% level of significance. To improve readability, letters were omitted when no significant difference was detected between means.

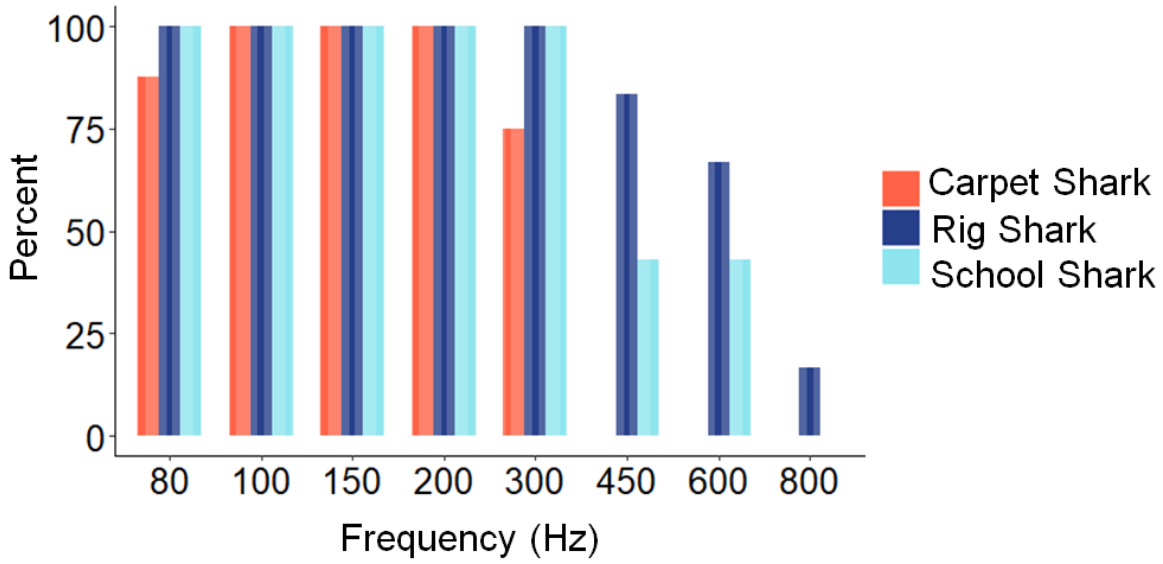

Fig. 8. Percentage of sharks that showed AEP responses to acoustic stimuli from an underwater speaker at each test frequency. Note that almost all sharks (19 of 20) across the three species responded from 80 Hz to 200 Hz, whereas fewer individuals responded to frequencies above 200 Hz AEPs, even at highest sound pressure levels evaluated.

Table 1. Sharks used for AEP measurements with an underwater speaker. Age class was assigned based on the average total length (TL) at maturity published for the carpet shark [male ~60 cm/ female ~75 cm (Horn, 2016)], rig shark [male ~85 cm/ female ~100 cm (Francis & Francis, 1992)], and school shark [male ~125-135 cm/ female ~135-140 cm (Francis & Mulligan, 1998)].

Species	ID	Sex	Total length (cm)	Age class
Carpet Shark (*Cephaloscyllium isabellum*)	T-CS5	male	58.5	juvenile
	T-CS3		63.5	adult
	T-CS9		62.8	
	T-CS1		65	
	T-CS8		67	
	T-CS7	female	70	juvenile
	T-CS6		70.5	
	T-CS4		75	
Rig Shark (*Mustelus lenticulatus*)	T-Rig6	male	51.5	juvenile
	T-Rig5		53.5	
	T-Rig9		56.8	
	T-Rig7	female	62	
	T-Rig8		67	
	T-Rig10		70	
School Shark (*Galeorhinus galeus*)	T-School3	male	49.5	juvenile
	T-School1		51.3	
	T-School5		58.5	
	T-School7		63.5	
	T-School4	female	58	
	T-School6		72.5	
	T-School2		73.5	

Table 2. Parameters of acoustic pip signals used in this experiment.

Frequency (Hz)	Duration (ms)	Hanning window[1] (ms)	Presentation rate (sec^{-1})	Recording window (ms)	Start SPL_{rms} (dB re: 1 µPa)	Start PAL_{rms} (dB re: 1 $µms^2$)
80	50	3	8	100	142.3	97.4
100					140.7	94.6
150					151.7	104.4
200					150.7	100.5
300					149	103.5
450	25				149.6	113
600					149.9	114.2
800					150	113.4
1200					151.1	117.8

[1]Time applies for rise, fall and plateau respectively.

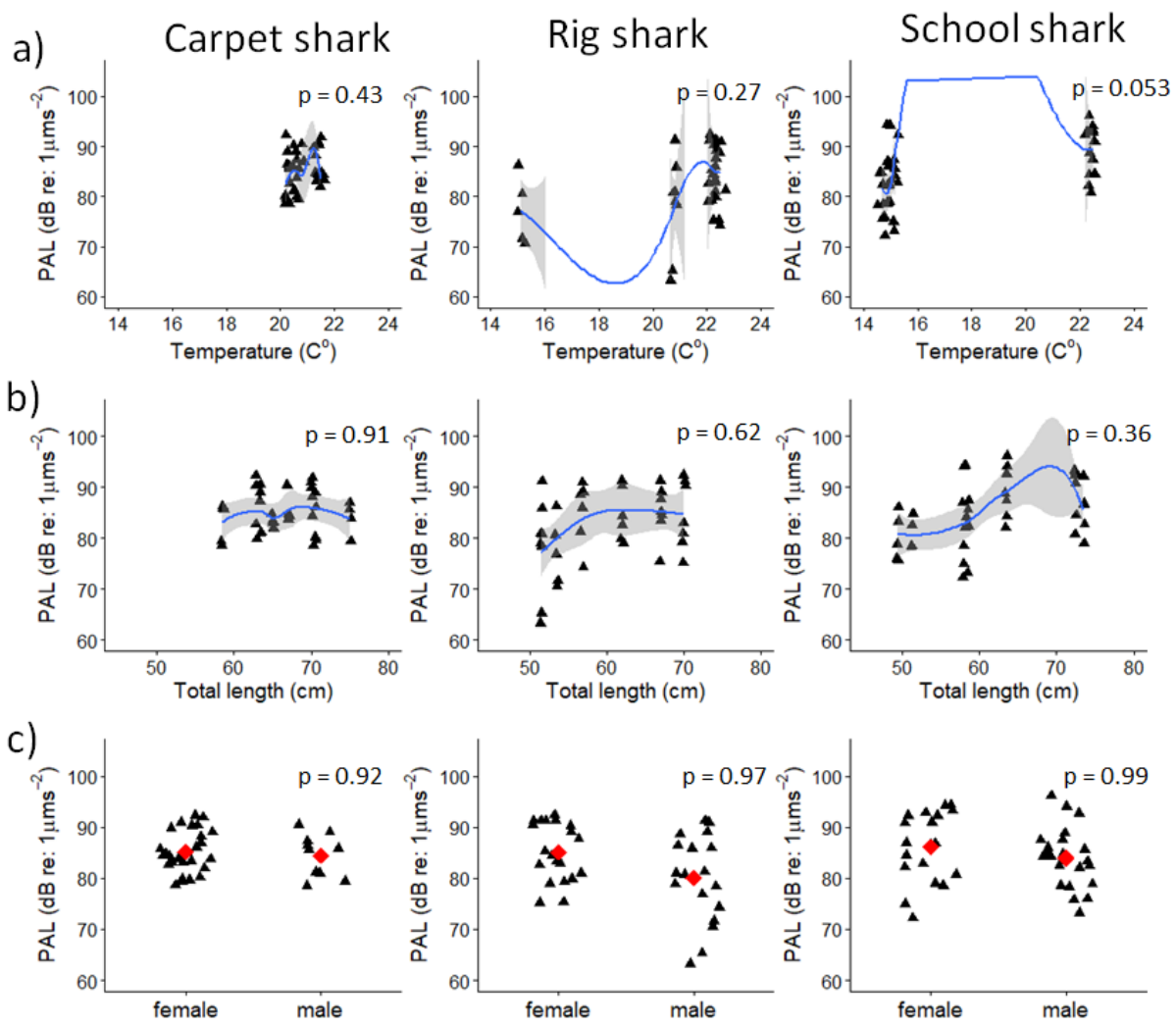

Fig. S1. Test for relationships of AEP thresholds with (a) water temperature, (b) total length, and (c) sex of the shark. Models were run to check for both liner and quadratic curve relationships. Note none of the associations were statistically significant.

Table S1. Post-hoc pairwise comparisons of visually and statistically derived pressure thresholds (dB re: 1 µPa SPL_{rms}).

Frequency	Species	Contrast	Estimate	SE	DF	t-ratio	p-value
80	Carpet.Shark	Carpet.Shark_80_statistical-Carpet.Shark_80_visual	-4.280	2.562	178	-1.67	0.0965
	Rig.Shark	Rig.Shark_80_statistical-Rig.Shark_80_visual	-5.047	2.767	178	-1.82	0.0698
	School.Shark	School.Shark_80_statistical-School.Shark_80_visual	-5.281	2.562	178	-2.06	0.0407
100	Carpet.Shark	Carpet.Shark_100_statistical-Carpet.Shark_100_visual	-5.484	2.396	178	-2.29	0.0233
	Rig.Shark	Rig.Shark_100_statistical-Rig.Shark_100_visual	-4.710	2.767	178	-1.70	0.0904
	School.Shark	School.Shark_100_statistical-School.Shark_100_visual	-4.773	2.562	178	-1.86	0.0641
150	Carpet.Shark	Carpet.Shark_150_statistical-Carpet.Shark_150_visual	-4.019	2.396	178	-1.68	0.0953
	Rig.Shark	Rig.Shark_150_statistical-Rig.Shark_150_visual	-3.588	2.767	178	-1.30	0.1963
	School.Shark	School.Shark_150_statistical-School.Shark_150_visual	-3.519	2.562	178	-1.37	0.1713
200	Carpet.Shark	Carpet.Shark_200_statistical-Carpet.Shark_200_visual	-1.656	2.396	178	-0.69	0.4903
	Rig.Shark	Rig.Shark_200_statistical-Rig.Shark_200_visual	-5.535	2.767	178	-2.00	0.0470
	School.Shark	School.Shark_200_statistical-School.Shark_200_visual	-4.759	2.562	178	-1.86	0.0649
300	Carpet.Shark	Carpet.Shark_300_statistical-Carpet.Shark_300_visual	-3.072	2.767	178	-1.11	0.2684
	Rig.Shark	Rig.Shark_300_statistical-Rig.Shark_300_visual	1.185	2.767	178	0.43	0.6690
	School.Shark	School.Shark_300_statistical-School.Shark_300_visual	-3.977	2.562	178	-1.55	0.1223
450	Rig.Shark	Rig.Shark_450_statistical-Rig.Shark_450_visual	-4.428	3.031	178	-1.46	0.1458
	School.Shark	School.Shark_450_statistical-School.Shark_450_visual	-5.593	3.913	178	-1.43	0.1546
600	Rig.Shark	Rig.Shark_600_statistical-Rig.Shark_600_visual	-3.992	3.389	178	-1.18	0.2403
	School.Shark	School.Shark_600_statistical-School.Shark_600_visual	-6.777	3.913	178	-1.73	0.0850

Table S2. Post-hoc pairwise comparisons of visually and statistically derived PAL thresholds (dB re: 1 µms^{-2} PAL$_{rms}$).

Frequency	Species	Contrast	Estimate	SE	DF	t-ratio	p-value
80	Carpet.Shark	Carpet.Shark_80_statistical-Carpet.Shark_80_visual	-4.280	1.886	178	-2.27	0.0245
	Rig.Shark	Rig.Shark_80_statistical-Rig.Shark_80_visual	-4.088	2.038	178	-2.01	0.0463
	School.Shark	School.Shark_80_statistical-School.Shark_80_visual	-4.716	1.886	178	-2.50	0.0133
100	Carpet.Shark	Carpet.Shark_100_statistical-Carpet.Shark_100_visual	-5.484	1.765	178	-3.11	0.0022
	Rig.Shark	Rig.Shark_100_statistical-Rig.Shark_100_visual	-5.242	2.038	178	-2.57	0.0109
	School.Shark	School.Shark_100_statistical-School.Shark_100_visual	-6.451	1.886	178	-3.42	0.0008
150	Carpet.Shark	Carpet.Shark_150_statistical-Carpet.Shark_150_visual	-4.019	1.765	178	-2.28	0.0240
	Rig.Shark	Rig.Shark_150_statistical-Rig.Shark_150_visual	-4.518	2.038	178	-2.22	0.0279
	School.Shark	School.Shark_150_statistical-School.Shark_150_visual	-7.066	1.886	178	-3.75	0.0002
200	Carpet.Shark	Carpet.Shark_200_statistical-Carpet.Shark_200_visual	-2.655	1.765	178	-1.50	0.1342
	Rig.Shark	Rig.Shark_200_statistical-Rig.Shark_200_visual	-4.912	2.038	178	-2.41	0.0169
	School.Shark	School.Shark_200_statistical-School.Shark_200_visual	-4.671	1.886	178	-2.48	0.0142
300	Carpet.Shark	Carpet.Shark_300_statistical-Carpet.Shark_300_visual	-3.072	2.038	178	-1.51	0.1335
	Rig.Shark	Rig.Shark_300_statistical-Rig.Shark_300_visual	1.243	2.038	178	0.61	0.5425
	School.Shark	School.Shark_300_statistical-School.Shark_300_visual	-3.919	1.886	178	-2.08	0.0392
450	Rig.Shark	Rig.Shark_450_statistical-Rig.Shark_450_visual	-3.680	2.232	178	-1.65	0.1010
	School.Shark	School.Shark_450_statistical-School.Shark_450_visual	-5.407	2.882	178	-1.88	0.0623
600	Rig.Shark	Rig.Shark_600_statistical-Rig.Shark_600_visual	-3.075	2.496	178	-1.23	0.2195
	School.Shark	School.Shark_600_statistical-School.Shark_600_visual	-6.880	2.882	178	-2.39	0.0180

Table S3. Post-hoc pairwise comparisons of statistically derived pressure thresholds (dB re: 1 µPa SPL_{rms}).

Frequency	Contrast	Estimate	SE	DF	t-ratio	p-value	p-adj.
80	Carpet.Shark_80-Rig.Shark_80	6.883	3.845	59.2	1.79	0.0785	0.1421
	Carpet.Shark_80-School.Shark_80	6.268	3.691	59.4	1.70	0.0947	0.1421
	Rig.Shark_80-School.Shark_80	-0.615	3.877	56.4	-0.16	0.8745	0.8745
100	Carpet.Shark_100-Rig.Shark_100	2.155	3.763	56.4	0.57	0.5691	0.7968
	Carpet.Shark_100-School.Shark_100	3.158	3.606	56.4	0.88	0.3849	0.7968
	Rig.Shark_100-School.Shark_100	1.003	3.877	56.4	0.26	0.7968	0.7968
150	Carpet.Shark_150-Rig.Shark_150	6.608	3.763	56.4	1.76	0.0845	0.1268
	Carpet.Shark_150-School.Shark_150	-1.122	3.606	56.4	-0.31	0.7569	0.7569
	Rig.Shark_150-School.Shark_150	-7.729	3.877	56.4	-1.99	0.0510	0.1268
200	Carpet.Shark_200-Rig.Shark_200	4.765	3.763	56.4	1.27	0.2106	0.3159
	Carpet.Shark_200-School.Shark_200	-1.004	3.606	56.4	-0.28	0.7818	0.7818
	Rig.Shark_200-School.Shark_200	-5.769	3.877	56.4	-1.49	0.1423	0.3159
300	Carpet.Shark_300-Rig.Shark_300	-3.465	3.951	62.7	-0.88	0.3838	0.5756
	Carpet.Shark_300-School.Shark_300	-4.393	3.802	63.2	-1.16	0.2522	0.5756
	Rig.Shark_300-School.Shark_300	-0.928	3.877	56.4	-0.24	0.8117	0.8117
450	Rig.Shark_450-School.Shark_450	-1.325	4.752	81.5	-0.28	0.7811	0.7811
600	Rig.Shark_600-School.Shark_600	-1.123	4.923	84.9	-0.23	0.8201	0.8201

Table S4. Post-hoc pairwise comparisons of statistically derived PAL thresholds (dB re: 1 μms^{-2} PAL_{rms}).

Frequency	Contrast	Estimate	SE	DF	t-ratio	p-value	p-adj.
80	Carpet.Shark_80-Rig.Shark_80	5.017	2.399	59.9	2.09	0.0407	0.122
	Carpet.Shark_80-School.Shark_80	3.271	2.303	60.2	1.42	0.1607	0.241
	Rig.Shark_80-School.Shark_80	-1.746	2.418	57.1	-0.72	0.4732	0.473
100	Carpet.Shark_100-Rig.Shark_100	4.458	2.348	57.1	1.90	0.0626	0.188
	Carpet.Shark_100-School.Shark_100	3.013	2.250	57.1	1.34	0.1858	0.279
	Rig.Shark_100-School.Shark_100	-1.445	2.418	57.1	-0.60	0.5524	0.552
150	Carpet.Shark_150-Rig.Shark_150	7.999	2.348	57.1	3.41	0.0012	0.004
	Carpet.Shark_150-School.Shark_150	2.954	2.250	57.1	1.31	0.1945	0.194
	Rig.Shark_150-School.Shark_150	-5.045	2.418	57.1	-2.09	0.0414	0.062
200	Carpet.Shark_200-Rig.Shark_200	5.534	2.348	57.1	2.36	0.0219	0.052
	Carpet.Shark_200-School.Shark_200	0.309	2.250	57.1	0.14	0.8913	0.891
	Rig.Shark_200-School.Shark_200	-5.225	2.418	57.1	-2.16	0.0349	0.052
300	Carpet.Shark_300-Rig.Shark_300	-0.233	2.466	63.5	-0.09	0.9251	0.925
	Carpet.Shark_300-School.Shark_300	-0.473	2.373	64.0	-0.20	0.8425	0.925
	Rig.Shark_300-School.Shark_300	-0.241	2.418	57.1	-0.10	0.9211	0.925
450	Rig.Shark_450-School.Shark_450	-5.099	2.969	82.1	-1.72	0.0897	0.090
600	Rig.Shark_600-School.Shark_600	-4.223	3.077	85.5	-1.37	0.1735	0.173

Table S5.

Click here to download Table S5